Journal of Photochemistry & Photobiology A: Chemistry 371 (2019) 25–32

Contents lists available at ScienceDirect

Journal of Photochemistry & Photobiology A: Chemistry

journal homepage: www.elsevier.com/locate/jphotochem

# Influence of synthesis conditions on the properties of photocatalytic titania-silica composites

Y. Hendrix, A. Lazaro, Q.L. Yu*, H.J.H. Brouwers

*Department of the Built Environment, Eindhoven University of Technology, P.O. Box 513, 5600 MB, Eindhoven, The Netherlands*

ARTICLE INFO

*Keywords:*
Photocatalysis
Titania-silica composite
NO oxidation
Precipitation
Sol-gel
Synthesis condition optimization

ABSTRACT

Titania-silica composites are a promising alternative to titania for photocatalysis, because of their lower material costs, longer lifetimes and higher activities. Different synthesis routes for titania-silica composites were thoroughly investigated in this study to gain more fundamental insight on their impact on the resulting samples and their photocatalytic oxidation efficiency. The investigated routes were based on precipitation, slow addition of an alkoxide precursor and sol-gel method. The silica for the composites was synthesized by dissolving the silicate mineral olivine in sulfuric acid. This method is cheaper, environmentally friendly and produces silica with favorable properties (i.e. large surface area with a high hydroxyl density) to support the titania. The resulting samples were tested by measuring their efficiency to oxidize nitric oxide under UV-light irradiation, XRD, nitrogen physisorption, FTIR and XPS. The results show that the most active photocatalysts were prepared by precipitation by slow addition of water or slow addition of precursor to a low water content dispersion. In addition, an optimal pH of 3 was observed for these synthesis methods. Compared to pure titania, the prepared titania-silica composites with only 15% titania showed slightly higher photocatalytic activities (82.3% vs. 78.9%), showing the composites to be a promising cost-effective alternative to the current photocatalysts.

## 1. Introduction

Due to their promising properties as photocatalysts, the number of studies on different titania-silica composites in the last decades has been enormous and is still growing [1–9]. Despite the non-photocatalytic nature of silica, the composites can have superior activity by enhanced adsorption properties [1–9]. Furthermore, due to the higher stability of silica, the lifetime of the composites is inclined to outperform that of pure titania. It has been shown that the anatase-rutile transformation happens at higher temperatures when the titania is bonded to silica [8]. This increase in energy requirement shows that the silica anchors the titania atoms in place, making it harder for the atoms to rearrange themselves into a lower active photocatalytic crystal lattice or to be removed, and thus, the bond to the silica increases the durability of the photocatalyst. In addition to enabling a higher photocatalytic activity and durability, the production cost of the composites can be greatly reduced when most of the bulk titania is replaced with a lower cost silica prepared by a sustainable synthesis method. Overall, the potentially higher performance, higher durability and lower cost of the composites make them more attractive for engineering applications like photocatalytic building materials [10–12].

The synthesis method used for the composites is crucial as it determines the titania morphology and the chemical bonding between the titania and the silica [1–8,13–15]. The photocatalytic advantages of the composites over pure titania are dependent on these two properties and on the morphology of the silica itself. For a high photocatalytic conversion, the coated titania should be crystalline, a few nanometers thin and homogenously distributed on the surface of the silica substrate. Due to the complexity of the coating mechanisms, many different approaches to prepare the composites are possible, but the ones that have a strong potential to form a cost-efficient photocatalyst are utilizing the hydrolysis-condensation reactions [3–5,26]. These methods are more flexible in approach, do not involve extreme temperatures and can form more than one monolayer in contrast to methods like impregnation and deposition. Three commonly used methods following the hydrolysis-condensation reactions are the precipitation method, sol-gel method and a method which uses slow addition of a titanium alkoxide precursor. These methods have their own advantages and disadvantages, resulting in composites with different properties.

While the synthesis method is crucial, the relationship between the methods and the properties of the resulting composites still needs more clarification. Many different studies have used a large variety of methods, resulting in a large range of composites [1–6]. Castillo et al. [2] has shown that the titania coating can be significantly different

* Corresponding author.
*E-mail address:* q.yu@bwk.tue.nl (Q.L. Yu).

https://doi.org/10.1016/j.jphotochem.2018.10.040
Received 22 June 2018; Received in revised form 19 October 2018; Accepted 23 October 2018
Available online 25 October 2018

depending on the preparation method. Nevertheless, the exact relationship between the applied synthesis method and the resulting photocatalytic behavior of each composite has not yet been reported. In addition, the large variety of applications, for which composites in literature have been prepared, makes it very difficult to relate the resulting properties of the composites with different methods. For example, Gao et al. [1] reported that up to 25 different photocatalytic reactions were applied in only 38 different studies about photocatalytic titania-silica composites. The activity of a photocatalyst can vary immensely with different reactions, since each targeted molecule for photocatalytic degradation or oxidation can have a different energy barrier, reduction potential, side-products and adsorption properties with the photocatalyst. For example, for the reduction of $CO_2$ into methanol [22] isolated $Ti^{3+}$ species are required while for the decomposition of methyl orange, a 5 nm layer of anatase was the most photocatalytic efficient titania structure [23].

To gain a better understanding between the direct relationship between coating method and resulting composite, a range of different synthesis routes was systematically investigated in this study. The three above mentioned methods, precipitation, addition and sol-gel methods, were applied with different variations, changing the relevant synthesis parameters to produce different $TiO_2$-$SiO_2$ composites to investigate their effects. The resulting photocatalytic properties of all composites were evaluated by testing their photocatalytic conversion of NO under UV-light using the ISO 22197-1 standard [16] for comparative purpose. Therefore, the selectivity issue of NOx oxidation is not addressed in this work. Furthermore, analytical techniques including, Fourier-transform infrared spectroscopy (FTIR), X-ray diffraction (XRD), X-ray photoelectron spectroscopy (XPS) and nitrogen physisorption, were used to thoroughly analyze the structure of the resulting composites.

## 2. Experimental methods

The silica used in this study was prepared by the dissolution of the silicate mineral olivine [17–21]. During this dissolution, the olivine and sulfuric acid react to form dissolved silica monomers following the reaction:

$$(Mg,Fe)_2SiO_4 + 4H^+ \rightarrow Si(OH)_4 + 2(Mg,Fe)^{2+} \quad (1)$$

The silica forms and precipitates after the critical supersaturation point of the silica monomers is reached. This silica is filtrated and washed with a diluted sulfuric acid solution to remove the remaining iron and magnesium ions and subsequently washed to remove the acid. The resulting product is a nano-structured silica with a large specific surface area of around 200 $m^2/g$, a particle size between 1 and 10 µm and a high hydroxyl density between 13 and 22 OH/$nm^2$ [17–21]. Before each experiment, the nano-silica was dried at 120 °C overnight. Subsequently, 20 g of the silica was weighed, milled and dispersed in the chosen dispersion medium to a total volume of 500 mL. Table 1 shows an overview of the parameters used in the experiments. In all experiments, the molar ratio of Ti:Si was kept at 15:85 to have an equal amount of titania, which was determined based our preliminary study. The precursors used were Titanium oxysulfate 15% in dilute sulfuric acid (Sigma-Aldrich), titanium (IV) isopropoxide 97% (Sigma-Aldrich) and a titania gel suspension (concentration 80%) produced from the sulfate process used for large scale nano-titania production (provided by Kronos). Each experiment with titanium oxysulfate started at a pH of 1 because of the sulfuric acid. After the composite synthesis, the resulting samples were filtered and washed four times with water. Afterwards, the samples were dried overnight at 120 °C and then calcined at 500 °C for four hours.

### 2.1. Precipitation method

During the precipitation method, the titanium precursor was first dissolved in the dispersion medium and then hydrolyzed by changing: pH, temperature or water content, making the titania precipitate on the silica. The samples Pr1 and Pr2 were synthesized at 20 °C by increasing the pH of the titanium oxysulfate solution using sodium hydroxide. The difference between these two experiments was that the method for Pr1 used water as the dispersion medium while the method for Pr2 used ethanol. No extra water was necessary for the hydrolysis of the titania precursor during the formation of Pr2, since the solution in which the precursor was dissolved already contained enough water. Pr3, Pr4 and Pr5 were synthesized by slowly increasing the temperature from 20 to 50, 70 and 90 °C, respectively. For the formation of Pr6, both the temperature and pH were increased. The preparations of Pr7 and Pr8 were done using titanium isopropoxide in ethanol as the dispersion medium without water so that hydrolysis was prevented by the absence of water. Afterwards, water was slowly added during 12 h until the water content of the dispersion medium reached 2.5 vol.%. For Pr8, the pH value was lowered to 3 by adding sulfuric acid (50 vol.%) in order to have a slower hydrolysis reaction and opposite charge between the silica and formed titania.

**Table 1**
Summary of the experiments performed in this study.

| Sample code | Precursor | Dispersion medium | pH | Temperature °C |
|---|---|---|---|---|
| Pr1 | TS | Water | *1→3 | 20 |
| Pr2 | TS | Ethanol | *1→7 | 20 |
| Pr3 | TS | Water | 1 | *50 |
| Pr4 | TS | Water | 1 | *70 |
| Pr5 | TS | Water | 1 | *90 |
| Pr6 | TS | Water | *1→3 | *50 |
| Pr7 | TP | Ethanol + * water | 7 | 20 |
| Pr8 | TP | Ethanol + * water | 3 | 50 |
| Ad1 | TP | Ethanol + water | 7 | 20 |
| Ad2 | TP | Ethanol + water | 3 | 20 |
| Ad3 | TP | Ethanol + water | 1 | 70 |
| Ad4 | TP | Ethanol + water | 3 | 50 |
| Sg1 | TP | Water | *7→2 | 20 |
| Sg2 | TG | Water | *7→2 | 20 |
| Sg3 | TS | water | *7→2 | 20 |

* = changed after adding the titanium precursor, → = changed into, Pr = precipitation method, Ad = slow addition method, Sg = Sol-Gel method, TS = titanium oxysulfate, TP = titanium isopropoxide and TG = titania gel.

### 2.2. Addition method

Applying the addition method, the titanium isopropoxide was slowly added to the silica-ethanol dispersions described in the general method section. The silica dispersions for the addition methods contained only 2.5 vol.% water with the rest being ethanol to have a slow hydrolysis rate. Ad1 was prepared at neutral pH and room temperature. The other three samples (Ad2-Ad4) were prepared at lower pH values using sulfuric acid in order to have even slower hydrolysis. A pH value of 3 was used for Ad2 and Ad4, and a value of 1 for Ad3. To increase the yield, the temperature of the dispersion medium was set as 70 °C and 50 °C for Ad3 and Ad4, respectively.

### 2.3. Sol-gel method

For the preparation of the sol-gel method samples, the titanium gels were first made and then added to the silica dispersions. Three different sources for the gel were investigated, as shown in Table 1. The gel for Sg1 was prepared by adding titanium isopropoxide to water; the gel for Sg2 was premade and provided by Kronos and the titania gel for Sg3 was made by rapid neutralization of titanium oxysulfate with sodium hydroxide, after which it was first washed and dried to remove the sodium and sulfate ions. Subsequently, the pH was lowered to 2 with sulfuric to form the composites. Sulfuric acid is able to catalyze the hydrolysis of the surface of the hydrated gel, forming titanium

hydroxide monomers and smaller polymers referred to as sol. Afterwards, three different reactions are possible: the sol binds again to the amorphous titania gel, it binds to the silica surface or it forms crystalline titania. Since amorphous titania is thermodynamically more soluble than the silica-bonded titania and the crystalline titania, the latter two will be favored over time just like in the Ostwald ripening process.

### 2.4. Analytical methods

The crystalline structures of the composites were measured using a XRD equipment with a Cu Kα source at 40 kV and 30 mA in steps of 0.02° every 8 s. The crystal size of anatase was determined using the Scherrer equation:

$$L = \frac{K\lambda}{\beta\cos\theta} \quad (2)$$

where L is the crystal size (m), K particle shape factor (0.89 was used), λ wavelength of the used X-ray, β width of a peak at half the maximum intensity in radians and θ corresponding peak angle. An approximation on the average size of the measured crystal structure can be calculated using this equation because the width of the XRD peaks depends on this value if the material consists of nano-sized crystals. In addition, nitrogen physisorption was performed with a Tristar II instrument to determine the specific surface area using the BET theory. Also, XPS measurements were performed to determine the Ti:Si ratio on the surface of the composites. They were performed with a Thermo Scientific K-Alpha using an Al Kα source of 1486.6 eV at 72 W measuring spots with the size of 400 µm at a reduced pressure.

FTIR measurements were performed using a Perkin Elmer spectrometer model Frontier with a resolution of 2 $cm^{-1}$. A small amount of the samples was first heated to 850 °C to remove all surface silanol groups since their IR absorption corresponds close to the Ti-O-Si bond absorption [24]. An example of the FTIR spectra is shown in Fig. 1. Because of the low titania amount, the Ti-O-Si is not clearly visible. To compare the bonding composition at the surface of the different samples, the following equation was used to calculate the ratio between the Ti-O-Si bond absorption and Si-O-Si bond absorption;

$$\text{bond ratio} = \frac{A_{Ti-O-Si}}{A_{Si-O-Si}} \quad (3)$$

where $A_{Ti\text{-}O\text{-}Si}$ is the sum of the absorption around the Ti—O—Si bond peak between 900-975 $cm^{-1}$ and $A_{Si\text{-}O\text{-}Si}$ the sum of the absorption around the Si—O—Si bond peak between 975-1300 $cm^{-1}$. If this bond ratio is high, it means that the titania is well-bonded to the silica.

### 2.5. Photocatalytic conversion measurement and NO adsorption

To compare the photocatalytic properties of all synthesized titania-silica composites, their photocatalytic conversion ability was determined by oxidizing the pollutant NO under UV-light irradiation. Photocatalytic oxidation of NO under UV-light produces $NO_2$, $HNO_2$ and $HNO_3$. The produced $NO_2$ and $HNO_2$ are likely to be further oxidized into $HNO_3$ by further photocatalytic oxidation if they are adsorbed near the photocatalyst. Due to photoexcitation, the surface of titania can cause the production of hydroxyl radicals ($OH^{\cdot}$) and superoxide radicals ($O_2^{\cdot-}$) [3], which are highly reactive and can oxidize NO into the mentioned products. The photocatalytic efficiency of the samples was determined by measuring how much of a continuous inflow of NO gas was oxidized following the standard ISO 22197-1 [16]. The setup for these measurements is shown in Fig. 2. In addition to the composites, a reference photocatalyst (P25, supplied by Evonik) was evaluated, both pure and mixed with dried silica under the same molar ratio (15:85). For a standard measurement, one gram of the samples was milled and dispersed in 10 mL water. This dispersion was then slowly dropped onto one side of a glass plate (200 mm × 100 mm) and with the use of a glass rod fully spread over its surface. Subsequently, these glass plates were dried at room temperature overnight. Whether the powdered coating obtained enough cohesion was tested by hanging the glass plates up-side down. Afterwards, the coated glass plates were put in the reactor with 3 mm of space between the top of the reactor and the glass plate. Through this gap, an air flow of 3 L/min was maintained with a NO inlet concentration of 1 ppm at ambient temperature of about 20 ± 1 °C. The relative humidity of the gas flow was kept constant at 50% using a bottle of water through which a controllable amount of the gas was pumped. During the photocatalytic oxidation (PCO) measurements, the samples were illuminated with UV-light with an intensity of 10 $W/m^2$. The NO pollutant, with the desired concentration by mixing with the synthetic air and desired humidity by flowing through a water bottle, first flows through a bypass in order to reach a stable condition. Afterwards, the NO is flowing through the reactor by switching off the bypass for about 10 min. without illumination to reach equilibrium because of surface adsorption. Then the reactor is illuminated for 2 h to reach a stable NO oxidation rate. The PCO conversion of NO was determined by the concentration difference between the inlet and outlet, applying the following equation:

$$\text{NO oxidation conversion (\%)} = 100(1\text{-}C_{NO\text{-}outlet}/C_{NO\text{-}inlet}) \quad (4)$$

where $C_{NO\text{-}outlet}$ is the average concentration of NO during the last 5 min of the PCO test during the UV illumination and $C_{NO\text{-}inlet}$ the average concentration of NO during 5 min before the illumination started.

The NO adsorption on the surface of the photocatalyst was

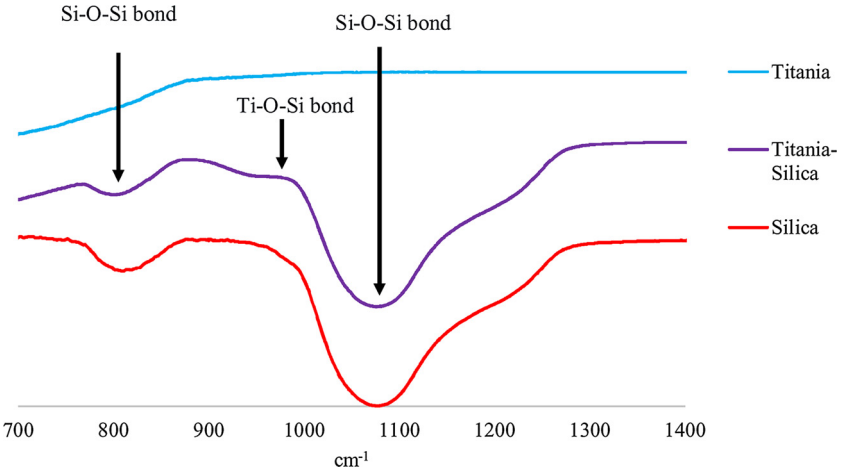


**Fig. 1.** FTIR spectra of bare $TiO_2$, bare $SiO_2$ and a composite sample (Pr7).

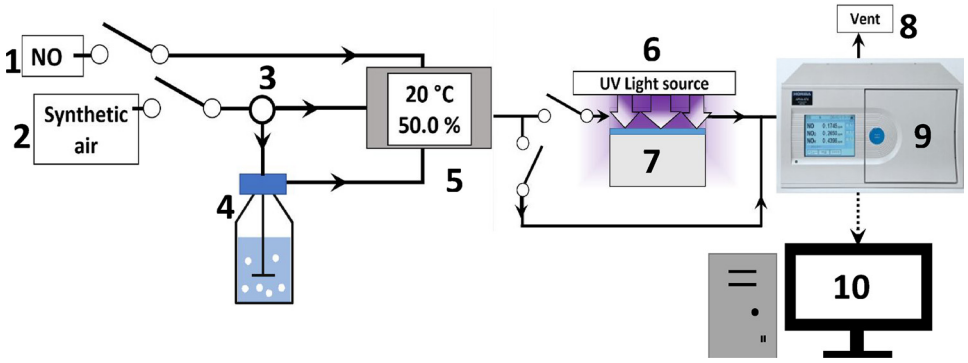


**Fig. 2.** Schematic view of the PCO measurement setup: 1) NO gas source, 2) synthetic air source, 3) valve, 4) bottle containing water, 5) humidity and temperature sensor, 6) light source, 7) reactor, 8) air vent, 9) NOx detector and 10) computer to control inflow of gasses and data collection.

estimated by using the difference in concentration between the 10 min of NO flow through the bridge and the 10 min through the reactor. This difference is caused by a drop in NO concentration caused by the filling of the reactor and NO adsorption on the photocatalyst. Thus, the total adsorption of NO on the surface of the photocatalyst can be estimated by subtracting the mass of NO in the reactor from the accumulated mass difference of the NO after the gas flow is derived to the reactor until equilibrium was reached.

## 3. Results analysis

It is important to note that every parameter in the evaluation method to determine the NO conversion can have an enormous impact on the photocatalytic oxidation efficiency [1]. For example, the substrate used on which the photocatalyst is anchored can greatly alter the $NO_x$ abatement by influencing the pollutant adsorption, the product adsorption, air flow (as was shown by Gauvin et al. [25]) and light adsorption [4]. To eliminate influence from the substrate and assess primarily the synthesized photocatalysts, a relatively high amount of photocatalyst was used on a smooth glass surface to have as little as possible contact between the glass substrate and the pollutants. Since the photocatalytic oxidation of NO was only performed for comparative reasons, while the applied substrate including microstructure and morphology significantly affects the selectivity of the produced $NO_2$ for further oxidation that requires an extensive investigation itself, it was chosen to show only the average NO oxidation efficiencies in this paper.

### 3.1. Precipitation composites

The results of the precipitation samples and their pH values are shown in Table 2. The results show that the pH has a significant effect on the resulting composites by influencing two main properties; besides the hydrolysis-condensation rates, it also influences the electrical charge on the silica surface and the formed titania. As Sugimoto et al. [26] reported, the formed titania monomers complexes ($Ti(OH)_n^{(4-n)+}$) change with different pH values. The majority of the monomers consist of $Ti(OH)_4$ at pH > 4, $Ti(OH)_3^+$ at a pH between 2 and 4 and $Ti(OH)_2^{2+}$ at pH < 2. In addition, the isoelectric point of silica is at a pH of around 1–2 and that of titania at a pH of around 4–5. Therefore, if the pH of the dispersion medium is between 2 and 4, the silica and titania are oppositely charged. Otherwise, the charges are either positive (pH < 2) or both negative (pH > 5). An opposite charge increases the chance of the titania monomers and polymers to make contact and form bonds with the silica surface due to electrical attraction, and thus, increasing the coverage of the titania over the silica.

The samples Pr1 to Pr6, which were prepared at a starting pH of 1, had a low coverage, little bonding and a poor photocatalytic activity with low adsorption relative to the other two Pr samples, which is attributed to the pH value. These samples were prepared at a starting pH of 1 to prevent the hydrolysis reaction during the dissolution of the precursor. However, it might be that because of the electrical repulsion, the titania nucleated in the solution instead of on the silica particles, which is thermodynamically favorable under conditions without repulsion.

While the pH was increased during the preparation of Pr1, Pr2 and Pr6, the neutralization process did not raise the pH instantaneously to a more favorable pH value. Therefore, the initial nucleation happens while there is still charge repulsion between the formed titania and silica. If the neutralization happened faster, the hydrolysis reaction would have been too rapid for controlled condensation. Compared to Pr1, it is shown that changing the dispersion medium to ethanol did not contribute to an enhanced efficiency (Pr2).

Due to the high stability of the precursor at low pH values, Pr3, Pr4 and Pr5 had low yields during the titania reaction. Their yields were 1, 41 and 76 wt.% of the potential titania, respectively, as calculated with

$$Yield(\%) = \frac{Product\ weight - added\ silica}{Mol\ mass\ of\ TiO_2 \times moles\ precursor} \quad (5)$$

All other samples had yields close to 100%. The low yield comes from non-reacted titania precursor going through the filter during the washing. Therefore, it can be assumed that the titania content of Pr3

**Table 2**
Results of the precipitation samples.

| Sample code | pH used during synthesis | NO conversion (%) | NO Adsorption (μg) | BET SSA ($m^2/g$) | XPS Ti content (%) | Anatase crystal size (nm) | FTIR: Bond Ratio |
|---|---|---|---|---|---|---|---|
| Pr1 | 1→3 | 13.4 | 0.32 | 152.1 | 1.5 | 18 | 0.033 |
| Pr2 | 1→7 | 13.0 | 0.35 | 161.1 | 0.8 | 25 | 0.052 |
| Pr3 | 1 | 12.7 | 0.61 | 188 | 0.8 | 22 | 0.026 |
| Pr4 | 1 | 32.8 | 0.71 | 173.6 | 1.4 | 24 | 0.032 |
| Pr5 | 1 | 26.0 | 0.47 | 180.3 | 2.7 | 24 | 0.038 |
| Pr6 | 1→3 | 8.6 | 0.21 | 176.2 | 1.3 | 16 | 0.022 |
| Pr7 | 7 | 80.4 | 1.67 | 199.2 | 19.3 | 12 | 0.083 |
| Pr8 | 3 | 82.3 | 1.92 | 199.9 | 13.0 | 11 | 0.089 |

and Pr4 are very low, which explains their low PCO efficiencies. However, even with a much higher yield, Pr5 did not show a higher NO conversion than Pr4. For Pr5, the high temperature caused a better yield but it also caused hydrolysis to happen faster, which might have resulted in secondary nucleation, and consequently less titania growth on the silica surface. The low bond ratio as measured with FTIR and the low coverage from the XPS measurements support this hypothesis which will be further discussed in the following sections.

Pr7 and Pr8 show very high PCO activity, especially compared to samples Pr1-Pr6, as shown in Table 2. These two samples were prepared by slowly adding water to the system continuously. As reported by Park et al. [27], the hydrolysis reaction of titanium isopropoxide requires a certain minimum concentration of water to take place. During the formation of Pr7 and Pr8, the hydrolysis started after reaching the critical concentration. The hydrolysis reaction consumes water, and thus, its rate was controlled by the water addition speed. Therefore, if the water addition is slow enough, the concentration of titania monomers will stay below the critical supersaturation point so that secondary nucleation is prevented. Another reason these two samples showed a high PCO efficiency was that, before the water was added to the system, the precursor had a chance to react with the silanol groups on the silica surface [5]. This successful bonding between the silica and titania through Ti−O−Si covalent bonds in these two samples is confirmed by the FTIR results which showed a much higher bond ratio compared to the other six precipitation samples. For Pr8 made at a pH of 3, the charge attraction between the formed titanium hydroxides and the silica surface and higher precursor stability caused the photocatalytic activity of this composite to be even higher. The reason that Pr7, prepared at a pH of 7, still obtained the high bond ratio and high coverage is that at pH > 6 the titania monomers is $Ti(OH)_4$ [27], and thus, uncharged. In addition, the excellent properties of Pr7 confirm that bonding can still happen without the charge attraction between the titania and silica as long as the hydrolysis is slow enough.

### 3.2. Addition composites

The results of the samples which were made by slow addition of precursor are shown in Table 3. Ad1 showed a relatively high photocatalytic efficiency, which is in line with the reported studies using the same method [1]. Nevertheless, the method can be further improved as shown by the samples Ad2 and Ad4 which achieved higher conversions. Sample Ad2 that was made in a dispersion with pH 3 had a higher photocatalytic activity than Ad1, the sample prepared at a pH of 7, which might be related to the charge attraction at that pH value. The higher temperatures used during the preparation of Ad4 helped to achieve an even higher NO conversion. In contrast, Ad3 had a very low NO conversion rate compared to the other addition samples even with higher temperatures. The NO conversion of Ad2 and Ad4 are rather similar, although higher temperature results in a slightly higher conversion. This indicates that under this condition temperature does not play a significant role. Therefore, the clearly lower efficiency of Ad3 can be primarily attributed to the very low pH (1) which might have caused the same disadvantages as mentioned before for the Pr3, Pr4 and Pr5 samples namely; charge repulsion and a too fast hydrolysis induced temperature causing secondary nucleation. In addition, Ad3 shows that the high PCO efficiency of the other samples made by this method cannot be contributed solely to the use of the alkoxide precursor as Ad3 used the same precursor.

**Table 3**
Results of the addition samples.

| Sample code | NO conversion (%) | NO Adsorption (μg) | BET SSA ($m^2$/g) | XPS : Ti (%) | Anatase Crystal size (nm) | FTIR: Bond Ratio |
|---|---|---|---|---|---|---|
| Ad1 | 58.2 | 0.44 | 215.3 | 15.1 | 13 | 0.075 |
| Ad2 | 75.6 | 0.82 | 199 | 13.0 | 13 | 0.040 |
| Ad3 | 20.4 | 0.49 | 178.3 | 8.8 | 16 | 0.054 |
| Ad4 | 79.2 | 0.66 | 205.9 | 19.9 | 12 | 0.085 |

### 3.3. Sol-gel composites

Many studies have been performed on the formation of titania nanoparticles with the sol-gel method since the study of Bischoff et al. [28]. The preparation of titania-silica composites applying this method is also possible [29] but the amount of studies on it are still relatively limited. Still, much of the gained information from studies on the titania nanoparticle formation can be used for the titania-silica composites. For the sol-gel methods, a pH of 2 was chosen in order to enable the hydrolysis of the amorphous titania, and thus, the Ostwald ripening process to precipitate the titania-sol on the larger silica structures. In addition, pH 2 is close to the isoelectric point of silica. Without charge on the silica surface, there was no charge repulsion during the coating between the titania and silica, while there was charge repulsion between titania particles. Furthermore, the pH-dependent stability of the precursor had no influence on the coating during the sol-gel method, since it was hydrolyzed before, unlike with the other two methods. As Table 4 shows, the sol-gel sample Sg1, which was prepared with titanium isopropoxide, shows an unexpectedly low efficiency. The reason for this low performance might be that the propanol that is formed during the hydrolysis disrupted the hydrolysis of the gel. Since the gel was more stable, the Ostwald ripening process was less effective, causing a great amount of the titania gel to remain separated from the silica as confirmed by the low bond ratio determined by the FTIR analysis (see Table 4). The large drop in the specific surface area from 200 to lower than 160 $m^2$/g by only 15 at.% of the sample indicates very large and smooth titania particles.

On the other hand, Sg2 and Sg3 show excellent NO conversions, 68.9% and 61.3%, respectively. Anatase could even be measured before the calcination step. The difference in photocatalytic efficiency can be attributed to the bond ratio. While Sg3 shows a higher photocatalytic efficiency than Sg1, FTIR shows that it has a low amount of bonds formed between the titania and silica. In fact, the samples Sg1 and Sg3 show the same bond ratio, meaning that the titania formed small particles (as indicated by the significantly higher specific surface area than Sg1) but these small particles almost did not form bonds to the silica surface. The difference between Sg2 and Sg3 that caused this difference in bonding was the titania source. The gel for Sg2 was already in an acidic environment with a high water content (~80 wt.% water), meaning that the titania was more hydrated and acidified for a longer time, and thus, had a higher solubility. The titania gel for Sg3 was first washed, and thus, contained no organic molecules unlike the gel for Sg1 and less acid molecules inside the gel than Sg2. Therefore, the formed titania nanoparticles during the preparation of Sg3 had a more effective electric charge on their surface, and thus, were more stable. However, this extra stability might have been one of the reasons for the low bonding ratio of Sg3 as stable particles are less likely to form additional bonds, which also explains the larger specific surface area than Sg1.

### 3.4. P25 reference

The NO conversion of the reference sample (P25) mixed with silica is lower than the NO conversions of the samples Ad2, Sg2 and Sg3, as shown in Table 5. However, the conversions of these three samples are lower than the plain P25. On the other hand, Pr7, Pr8, and Ad4 have even higher conversions than that of pure P25. These results prove that titania-silica composites can be more photocatalytically efficient than pure titania, which can be explained by the improved adsorption capabilities close to the titania added by the silica if the titania is homogenously distributed over the silica [1–3]. Nevertheless, the lower PCO efficiencies of the other samples confirm the crucial role the

**Table 4**
Results of the sol-gel samples.

| Sample code | Gel source | NO conversion (%) | NO Adsorption (μg) | BET SSA ($m^2$/g) | XPS Ti content (%) | Anatase crystal size (nm) | FTIR: Bond Ratio |
|---|---|---|---|---|---|---|---|
| Sg1 | Titanium isopropoxide | 5.6 | 0.33 | 159.7 | 1.3 | 22 | 0.029 |
| Sg2 | Gel provided by Kronos | 68.9 | 0.22 | 198.3 | 3.9 | 20 | 0.082 |
| Sg3 | Titanium oxysulfate | 61.3 | 0.55 | 181 | 0.9 | 24 | 0.029 |

**Table 5**
Results of the reference, pure and mixed with the nano-silica in ratio.

| Sample code | NO conversion (%) | NO adsorption (μg) | BET SSA ($m^2$/g) | Crystal size (nm) |
|---|---|---|---|---|
| P25 | 78.9 | 0.29 | 50* | 21* |
| P25 + $SiO_2$ | 58.3 | 0.58 | – | 21* |

* Data acquired from supplier.

**Table 6**
Peak positions of the binding strength of electrons from oxygen and titanium.

| Sample code | O 1 s $SiO_2$ (eV) | O 1 s $TiO_2$ (eV) | Ti $2p_{2/3}$ (eV) | Ti $2p_{2/3}$ (eV) |
|---|---|---|---|---|
| Pr1 | 532.56 | 529.34 | 464.22 | 458.53 |
| Pr2 | 532.97 | – | 464.37 | 458.8 |
| Pr3 | 533.19 | – | 464.57 | 458.96 |
| Pr4 | 533.17 | – | 464.54 | 458.97 |
| Pr5 | 532.55 | 529.38 | 464.03 | 458.37 |
| Pr6 | 533.01 | – | 464.64 | 458.98 |
| Pr7 | 532.54 | 529.99 | 464.28 | 458.63 |
| Pr8 | 533.17 | 530.3 | 464.73 | 459.1 |
| Ad1 | 532.81 | 529.84 | 464.28 | 458.65 |
| Ad2 | 532.57 | 529.65 | 463.99 | 458.32 |
| Ad3 | 533.01 | 532.09 | 464.62 | 458.99 |
| Ad4 | 532.64 | 529.84 | 464.35 | 458.7 |
| Sg1 | 532.54 | – | 464.51 | 458.89 |
| Sg2 | 532.63 | 529.95 | 464.19 | 458.57 |
| Sg3 | 533.45 | 529.9 | 464.65 | 459.15 |

preparation method for the composites plays.

### 3.5. Binding energies

Further information the XPS could tell about the coating is the bonding strength related to binding energies of the electrons of the oxygen and titanium atoms. Since silicon has a lower shielding effect, the electrons of neighboring atoms have higher binding energies than those neighboring titanium atoms. Therefore, it is known that the binding energy of the 1 s electrons in oxygen atoms in a Ti—O—Si bond can shift the peaks of the oxygen electrons in titania (around 529 eV) and silica (around 532.5 eV). In addition, the electrons of the titanium atoms close to the silicon atoms are thought to show higher binding energies, causing another shift. These binding energies are shown in Table 6. Unfortunately, the electron binding energy shifts appear to be a bit random, which might be due to the relatively low titanium amounts causing most peak shifts to have a large deviation.

## 4. Discussions

The XPS results can be used to correlate with the PCO efficiency since XPS measures only the surface of the material where the photocatalytically active agent is coated. Fig. 3 shows that there is indeed an overall trend that with a higher surface titanium amount, the photocatalytic efficiency is higher.

The reason why all titanium surface fractions are below 20% as determined by XPS is explained by the low amount of titania. The specific surface area of the titania can only be 10% of that of the silica when their molar ratio is 15:85 if one takes the titania as free spheres with crystal size of 11 nm (Table 2) and compares it to the external specific surface area of the bare nano-silica (168 $m^2$/g). Using the density of anatase (3.9 g/$cm^3$) the calculated specific surface area is 16.4 $m^2$ per gram of $SiO_2$. However, the structure is much more complex, i.e. both the silica and titania surfaces are not smooth. In fact, the silica surface consists of nanoparticles agglomerated into larger structures [17–21]. Thus, the main reason for the higher values is that the assumptions made for the calculations are not entirely correct. For instance, not all titania is in the form of perfect monodisperse spherical crystals. This assumption was only made to be able to use The Scherrer equation. For this calculation it is assumed that the structure of the titania is smooth and spherical, which is in fact rough and irregular, and thus, can cover more surface area. In addition, the titania that is too amorphous due to having a too small crystal size is not measurable with XRD, causing the actual average size of the titania crystals to be potentially smaller. Another reason for the relatively high titanium amount in XPS is that the silica surface in large pores or silica surface

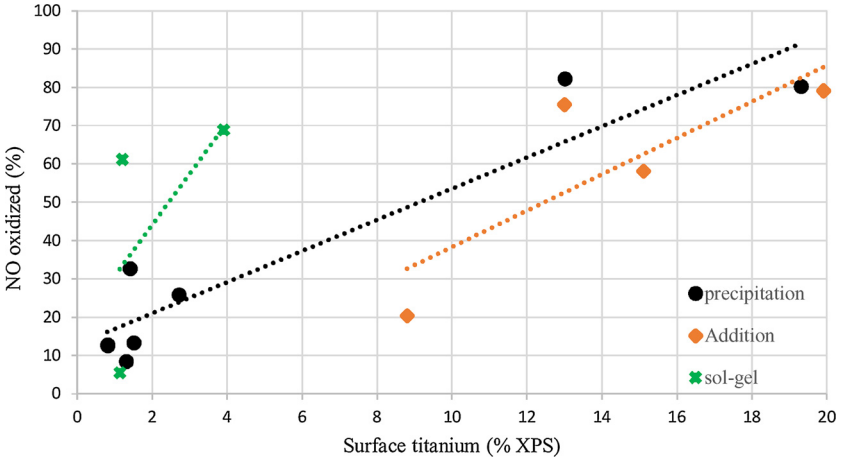


**Fig. 3.** Correlation between the titanium surface fraction as measured with XPS and the activity of the photocatalyst.

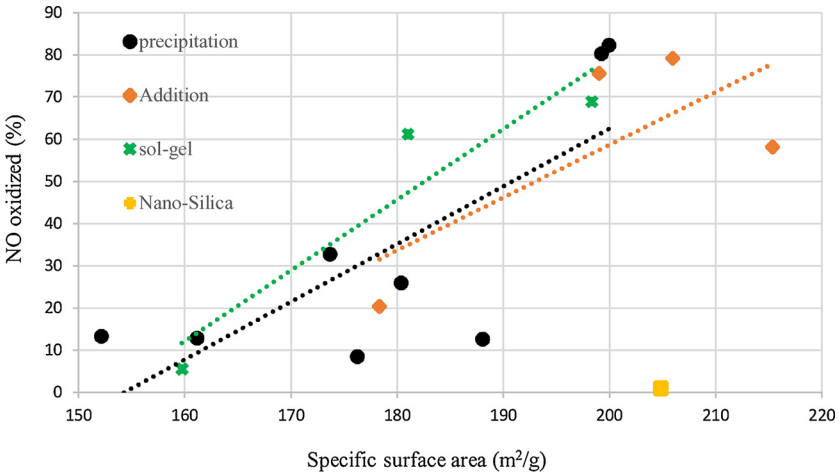


**Fig. 4.** Correlation between the surface areas of the composites and the NO oxidation of the photocatalyst.

covered by titania can not be measured with XPS. On the other hand, most of the samples showed titanium amounts below 4%, which was most likely because of imperfect coating whereby large titania agglomerates formed during the synthesis of these experiments, causing the low titanium amounts as determined with XPS and the low photocatalytic efficiencies.

The morphology of the formed titania affected not only the XPS results but also the specific surface area and bond ratio. Larger titania particles cause a smaller specific surface area. The surface area also correlates with the PCO efficiencies just like the titanium amount in the XPS results as shown in Fig. 4. The oxidation of NO does not require the NO molecules to be directly adsorbed onto the titania since the silica surface near the titania can also act as active sites [1,3,4]. Therefore, as long as the titania is well distributed over the silica, a larger external surface of the composites will have a higher amount of active sites, and thus, a higher photo-oxidation efficiency. Especially the difference in photocatalytic efficiency between Sg1 and Sg3 caused by the different morphology as explained in Section 3.3 shows a good example of this effect. This effect also explains why P25, with only a surface area of 50 $m^2/g$, had lower PCO efficiencies than the well-coated samples even though it had a 100% titania surface.

The differences in photocatalytic efficiency between some samples are relatively small. For example, the samples Pr7, Pr8, Ad2 and Ad4, which were all synthesized with the alkoxide precursor in a dispersion with low water content, all show promising results. However, the photocatalytic efficiencies of Pr2 and Ad3, which were also made with a relatively low water content, are almost insignificant showing that at pH 1 the coating does not work. However, the trends do not always predict the best photocatalysts. For instance, Ad2 and SG2 had a lower specific surface area and XPS titanium amount than Ad1, but a higher photocatalytic activity, indicating the system is very complex and future research is still needed. On the other hand, all the sol-gel samples are very different than both the precipitation and addition samples in terms of the end morphology since its method relies on a different chemical process. Due to the Ostwald ripening process of the titania at low pH, the final titania on the composite particles from the sol-gel method will be smoother and larger than with the other two methods. Therefore, the sol-gel samples had lower coverage and smaller specific surface areas, which in turn lead to lower photocatalytic efficiencies even with a high bond ratio like with Sg2. Despite this lower efficiency, the cost-efficiency of the sol-gel method is still potentially good due to the significantly lower costs of the precursor needed for this method.

## 5. Conclusions

This study shows that coating silica with titania can result in very promising photocatalysts. This newly synthesized photocatalysts show excellent photocatalytic activity, in terms of the NO oxidation, attributed to the large specific surface area, high amount of Ti-O-Si bonds, small crystal sizes of 10–20 nm and high titania coverage of the silica surface. The synthesis conditions, including three different methods and a number of critical parameters, on the photocatalytic efficiency were evaluated. The following conclusions can be reached:

- The pH plays the most important role for the investigated methods since it determines the precursor stability and the interaction between the silica and titania. All samples prepared at a pH value of 1 showed rather poor results.
- For both the precipitation and addition methods, the best results were obtained using a medium with a low water content and a pH value of 3. These resulting titania-silica composites with only 15 at. % titania are more photocatalytically efficient than the reference P25.
- The sol-gel method obtained the best result when used without organic solvents and with a fully hydrated and acidified titania gel. The resulting composite photocatalysts had lower efficiencies than of the other two methods but still higher than the reference P25 mixed with silica in the same ratio.
- While the samples prepared with the sol-gel method had lower photocatalytic efficiencies, the sol-gel method is more cost-effective since it is not limited to organic solvents as dispersion medium and titanium alkoxides as precursor.

## Acknowledgements

The authors wish to thank M.W.G.M. Verhoeven for performing the XPS measurements at the Department of Chemical Engineering and Chemistry of Eindhoven University of Technology (The Netherlands). Also Q. Alam is thanked for his help with writing. This study was performed as part of the STW project: Tailoring new nano-silica, and its application in smart concrete, project number 12824. We also thank the following companies for further sponsoring: Kronos International inc., Kijlstra Betonmortel, Graniet imort Benelux BV, Joma international, Selor eeig, ENCI BV and BAM.

## References

[1] X. Gao, I.E. Wachs, Catal. Today 51 (1999) 233–254.
[2] R. Castillo, B. Koch, P. Ruiz, B. Delmon, J. Mater. Chem. 4 (1994) 903–906.
[3] Y. Hendrix, A. Lazaro, Q.L. Yu, H.J.H. Brouwers, World J. Nano Sci. Eng. (2015) 161.
[4] A.Y. Shan, T.I.M. Ghazi, S.A. Rashid, Appl. Catal. A Gen. 389 (2010) 1–8.
[5] A. Hanprasopwattana, S. Srinivasan, A.G. Sault, A.K. Datye, Langmuir 12 (1996)

3173–3179.
[6] M. Montes, F.P. Getton, M.S.W. Vong, P.A. Sermon, J. Solgel Sci. Technol. 8 (1997) 131–137.
[7] Y. Xu, W. Zheng, W. Liu, J. Photochem. Photobiol. A: Chem. 122 (1999) 57–60.
[8] V.S. Smitha, K.A. Manjumol, K.V. Baiju, S. Ghosh, P. Perumal, K.G.K. Warrier, J. Solgel Sci. Technol. 54 (2010) 203–211.
[9] A. Fujishima, X. Zhang, D.A. Tryk, Surf. Sci. Rep. 63 (2008) 515–582.
[10] L. Pinho, M.J. Mosquera, Appl. Catal. B 134 (2013) 205–221.
[11] G. Hüsken, M. Hunger, H.J.H. Brouwers, Build. Environ. 44 (2009) 2463–2474.
[12] Q.L. Yu, H.J.H. Brouwers, Appl. Catal. B 92 (2009) 454–461.
[13] R. Van Grieken, J. Aguado, M.J. Lopez-Munoz, J. Marugán, J. Photochem. Photobiol. A: Chem. 148 (2002) 315–322.
[14] W.P. Hsu, R. Yu, E. Matijević, J. Colloid Interface Sci. 156 (1993) 56–65.
[15] R.H. Ryu, S.C. Kim, S.M. Koo, D.P. Kim, J. Solgel Sci. Technol. 26 (2003) 489–493.
[16] International Organization for Standardization, ISO 22197-1:2007, Switzerland.
[17] A. Lazaro, H.J.H. Brouwers, G. Quercia, J.W. Geus, Chem. Eng. J. 211 (2012) 112–121.
[18] A. Lazaro, M.C. Van de Griend, H.J.H. Brouwers, J.W. Geus, Microporous Mesoporous Mater. 181 (2013) 254–261.
[19] A. Lazaro, G. Quercia, H.J.H. Brouwers, J.W. Geus, World J. Nano Sci. Eng. 3 (2013) 41–51.
[20] A. Lazaro, L. Benac-Vegas, H.J.H. Brouwers, J.W. Geus, J. Bastida, Appl. Geochem. 52 (2015) 1–15.
[21] A. Lazaro, K. Sato, H.J.H. Brouwers, J.W. Geus, Microporous Mesoporous Mater. 267 (2018) 257–264.
[22] M. Anpo, H. Yamashita, K. Ikeue, Y. Fujii, S.G. Zhang, Y. Ichihashi, T. Tatsumi, Catal. Today 44 (1998) 327–332.
[23] T. Luttrell, S. Halpegamage, J. Tao, A. Kramer, E. Sutter, M. Batzill, Sci. Rep. 4 (2014) 4043.
[24] J.P. Launer, Silicone Compounds Register and Review 100 (1987).
[25] F. Gauvin, V. Caprai, Q. Yu, H.J.H. Brouwers, Appl. Catal. B 227 (2018) 123–131.
[26] T. Sugimoto, X. Zhou, A. Muramatsu, J. Colloid Interface Sci. 252 (2002) 339–346.
[27] H.K. Park, D.K. Kim, C.H. Kim, J. Am. Ceram. Soc. 80 (1997) 743–749.
[28] B.L. Bischoff, M.A. Anderson, Chem. Matters 7 (1995) 1772–1778.
[29] C.H. Kwon, J.H. Kim, I.S. Jung, H. Shin, K.H. Yoon, Ceram. Int. 29 (2003) 851–856.